Histopathology

Histopathology 2017, **71**, 125–133. DOI: 10.1111/his.13190

H3F3A mutation in giant cell tumour of the bone is detected by immunohistochemistry using a monoclonal antibody against the G34W mutated site of the histone H3.3 variant

Julian Lüke,[1,*] Alexandra von Baer,[2,*] Jordan Schreiber,[1] Christoph Lübbehüsen,[1] Thomas Breining,[3] Kevin Mellert,[1] Ralf Marienfeld,[1] Markus Schultheiss,[2] Peter Möller[1] & Thomas F E Barth[1]

[1]*Institute of Pathology, Ulm University,* [2]*Department of Surgery, Ulm University, and* [3]*Department of Radiology, Ulm University, Ulm, Germany*

Date of submission 11 November 2016
Accepted for publication 14 February 2017
Published online *Article Accepted* 17 February 2017

Lüke J, von Baer A, Schreiber J, Lübbehüsen C, Breining T, Mellert K, Marienfeld R, Schultheiss M, Möller P & Barth T F E

(2017) *Histopathology* **71**, 125–133. DOI: 10.1111/his.13190

H3F3A mutation in giant cell tumour of the bone is detected by immunohistochemistry using a monoclonal antibody against the G34W mutated site of the histone H3.3 variant

Aims: Giant cell tumour of the bone (GCTB) is a neoplasm predominantly of long bones characterized by the H3F3A mutation G34W. Conventional diagnosis is challenged by the tumour's giant cell-rich morphology, which overlaps with other giant cell-containing lesions of the bone. Recently, a monoclonal antibody specific for the H3F3A mutation has been generated. Our aim was to test this antibody on a cohort of giant cell-containing lesions.

Methods and results: We used the antibody for analysis of 22 H3F3A-mutated GCTB, including two patients with recurrences; for comparison we analysed a cohort of 36 H3F3A wild-type giant cell-rich lesions of the bone and soft tissue, containing one brown tumour, six aneurysmal bone cysts (ABC), six chondroblastomas, five non-ossifying-fibromas, two fibrous dysplasias, nine tenosynovial giant cell tumours, one giant cell-rich sarcoma and six osteosarcomas. Furthermore, among the 22 mutated cases, we included one GCTB with two recurrences and lung metastases; the patient was treated with the anti-receptor activator of nuclear factor κB (RANK) ligand denosumab. We show that all 22 H3F3A-mutated GCTB display strong nuclear H3.3 G34W staining in the neoplastic component, while the osteoclastic giant cells are negative. 36 H3F3A wild-type lesions are negative. The GCTB treated with denosumab revealed a reduction in the H3.3 G34W-positive tumour cells and a decrease in osteoclastic giant cells accompanied by matrix and osteoid formation.

Conclusions: We conclude that positive H3.3 G34W staining is a specific and sensitive method for detection of H3F3A-mutated GCTB. Denosumab treatment leads to a pathomorphosis of the lesion characterized by matrix and osteoid producing H3.3 G34W-negative stromal cells.

Keywords: G34W, giant cell tumour of bone, H3F3A mutation

Introduction

Giant cell tumour of the bone (GCTB) is a lesion characterized by mononuclear spindle-shaped neoplastic cells, interspersed with osteoclastic giant cells; GCTB is mainly a benign bone lesion which tends to grow at

Address for correspondence: Peter Möller, Institute of Pathology, M23 University of Ulm, Albert-Einstein-Allee 11, D-89081 Ulm, Germany. e-mail: peter.moeller@uniklinik-ulm.de
*These authors contributed equally to this study.

the end of long bones.[1] GCTB growth is locally aggressive, displaying osteolysis in both radiographic imaging and histomorphology.[2,3] Histological evaluation of GCTB has to differentiate this lesion from other giant cell-containing lesions that may have histological similarities with GCTB. The most frequently occurring benign mimics are aneurysmal bone cyst (ABC), chondroblastoma, non-ossifying fibroma (NOF), tenosynovial giant cell tumour (TSGCT) and the so-called brown tumour occurring in hyperparathyroidism.[4–6] Malignant lesions such as giant cell-rich osteosarcoma may resemble GCTB on histological grounds.[1,6] Aggressive GCTB with disease recurrence and sometimes even metastatic spread to the lungs have been described; while rare, this entity may be mistaken for giant cell-containing osteosarcoma.[7–9]

Histones are proteins that are important for DNA packaging. Variants of the histone H3 exist. Of these, variant H3.3 is encoded by two genes, H3F3A on chromosome 1 and H3F3B on chromosome 17.[10]

In 2013, a distinct driver mutation in the histone tail of the histone variant H3.3 was reported to be highly specific for GCTB and to occur in this tumour entity in up to 92% of GCTB analysed.[4,6,11] The mutation is restricted to the neoplastic spindle cell in GCTB, while the intermingled osteoclastic giant cells are negative for this mutation. Located on the H3F3A gene, it is responsible for an alteration of histone variant H3.3 leading to p.Gly34Tryp.[11] Recently, a monoclonal antibody (mAb) has been developed targeting the mutational site G34W of the histone variant H3.3. We have examined the potential of this antibody as diagnostic tool for the diagnosis of H3F3A-mutated GCTB by testing this antibody on a cohort of 64 samples of giant cell-rich bone and joint/soft tissue lesions which had been analysed beforehand using polymerase chain reaction (PCR)-based H3F3A mutational testing.

Material and methods

Using a diagnostic computer system, a collection of giant cell tumours of bone and other giant cell-rich lesions from a time-frame between 2002 and 2016 were retrieved from the paraffin archives. All methods and experiments performed were in line with the guidelines of the ethics committee of the Federal General medical Council.[12] The research was carried out in compliance with the Helsinki Declaration. All experimental protocols were conducted and approved in accordance with the local ethics committee of the University of Ulm (vote for usage of archived human material 03/2014).

Tissue samples were fixed in formalin pH 7.4. Bone tissue was decalcified using standard procedures with overnight incubation in ethylenediamine tetraacetic acid (EDTA) pH 7.4. To investigate the influence of different decalcification procedures, bone tissue of H3F3A-mutated GCTB was incubated alternatively with a mixture of HCl at 37%, formic acid at 99% and aluminium chloride and aqua destilata for 12 h and then embedded in paraffin for tissue section preparation. All samples were analysed for the mutational status of H3F3A as follows: a sequence of the H3F3A gene covering codon 34 in exon 2 was amplified from tissue extracted DNA by endpoint PCR using the M13-tailed primers H3F3A_for (5′-CGT TGT AAA ACG ACG GCC AGT GAA TTG TCA TGG CTC GTA CAA AGC AGA-3′) and H3F3A_rev (5′-GCA AAA AGT TTT CCT GTT ATC CA-3′). The resultant PCR product was subjected to Sanger sequencing using standard procedures.

The monoclonal rabbit antibody targeting the mutational site G34W on histone 3, variant H3.3 (clone RM263), used for immunohistochemistry (IHC) was provided by RevMab Biosciences (San Francisco, CA, USA). The antibody was diluted in antibody diluent (Zytomed Systems, Berlin, Germany) at a dilution of 1:400, as recommended by the manufacturer. In a pilot study, the optimal staining method was established as follows: the antibody was used on 2–3 μm formalin-fixed and paraffin-embedded tissue slides from four GCTB cases. Two of the four cases were known to be wild-type (WT) for H3F3A, while the other two had been shown to harbour the mutation G34W by means of sequencing. Immunohistochemistry (IHC) was performed following a standardized avidin–biotin–complex scheme and detection was achieved by chromogen RED (Dako, Hamburg, Germany). As antigen retrieval methods, the following heat-induced techniques were tested: steamer treatment, heating in a microwave oven and heating in a pressure cooker for a total of 20 min each. In the steamer treatment, buffers were either TRS/HCl with pH = 6.1, EDTA with pH = 8.0 or EDTA with pH = 9.0. Both microwave and pressure cooker treatment used citrate buffer with pH = 6.0.

After testing various concentrations and antigen retrieval methods, a dilution of 1:400 combined with EDTA buffer at pH = 8.0 and steamer treatment was found to deliver the best staining results with strongly stained nuclei in the samples, harbouring the H3F3A mutation. The rabbit mAb H3.3 K36M

detecting antibody (clone RM193), targeting the distinct histone mutation in chondroblastoma, was purchased from RevMAb (RevMAb Biosciences, San Francisco, CA, USA); staining a cohort of eight chondroblastomas was performed as published recently.[13] Fluorescence *in-situ* hybridization (FISH) was performed using standard protocols.[14] For FISH analysis of the USP-6 region a commercially available dual-colour break-apart probe was used for 17p13.2 (Zytovision, Bremerhaven, Germany). The presence of USP-6 rearrangement is a diagnostic criterion for ABC, a bone lesion also containing giant cells and sometimes mimicking GCTB. For evaluation of the extracellular matrix content, we used an Azan staining. Two of the group (T.F.B. and J.L.) evaluated IHC and matrix contents on a multihead microscope.

Results

Using the H3.3 G34W detecting antibody (clone RM263), we detected clear and strong staining in the nuclei of the mononuclear cell population of H3F3A mutated GCTB; staining was also positive on acid decalcified bone tissue. In contrast, all other nuclei of intermingled cell types, including the osteoclastic giant cells, were negative. A total of 64 samples were analysed immunohistologically using this antibody. The immunohistochemical staining pattern was suitable for identifying all samples that were initially tested positive for the H3F3A mutation ($n = 28$) by means of PCR and sequencing. The samples showed a strong and consistent nuclear staining in the stromal compartment, ranging from 10% to 90% of stromal nuclei (Table 1). It is noteworthy that in two patients with recurrences the primary tumour (case 21) and the resection sample of the head of the fibula (case 22) were negative regarding the H3F3A mutation. Immunohistological analyses of these samples, however, revealed between 10 and 40% of H3.3 G34W-positive cells. As the positive cell population in IHC was above 40% in all samples tested positively for G34W using Sanger sequencing, we conclude that the low numbers of neoplastic cells outnumbered by non-neoplastic cells were responsible for the negative sequencing results of the mutation analysis (Figure 1A, B).

By contrast, all cells in the brown tumour, ABC, chondroblastoma, NOF, TSGCT and two samples of fibrous dysplasia were completely negative (Supporting information, Figure S1; Table 2). Diagnosis of ABC was confirmed further by rearrangement of the USP6 region using FISH analyses, while all chondroblastomas were positive with immunohistochemistry using the rabbit mAb H3.3 K36M detecting antibody. One giant cell-rich high-grade sarcoma and six osteosarcomas were negative for staining with the H3.3 G34W antibody.

Furthermore, we analysed the tissue of one H3F3A mutated GCTB of the femur of a 29-year-old female patient, who developed bilateral pulmonary lesions 7 months after first diagnosis. Histological analyses and H3F3A mutational analyses of the initial lesions in the femur as well as the recurrences showed the H3F3A mutation in the tumour tissue. In April 2016 a computerised tomography (CT) scan (Figure 2C) of the thorax revealed multiple lesions in both lungs measuring up to 1.5 cm (up to 20 lesions in one lung each). An interdisciplinary sarcoma board of our institution decided to perform a lung biopsy. Histology of the lung biopsy showed a mononuclear infiltrate with intermingled osteoclast-like giant cells. Mutation analyses revealed a H3F3A mutation in the pulmonary lesion. Therefore, the lesion was regarded as lung metastasis of the GCTB of the femur. All tissue samples from the curettages and the tissue from the lung biopsy were strongly positive for H3.3 G34W in the nuclei of the stromal compartment of the GCTB (Figure 3A, A′). This led to the decision to begin denosumab therapy. The patient received four subcutaneous injections of 120 mg denosumab between May and July 2016. The tumour progressed around the bone cement implanted after curettage. Additionally, two soft tissue lesions measuring up to 2.5 cm around the femur showed progressive growth. Due to local disease progression, the distal femur was resected in August 2016. Pathological work-up confirmed the two lesions in the soft tissue around the distal femur. A further extra-articular lesion of 0.7 cm was detected in the ventral soft tissue. Tumour was also present around the curettage cave. Histological evaluation revealed a strong reduction of the osteoclastic giant cells in all but one of the extra articular lesions accompanied by a strand-like matrix formation (Figure 3C). H3.3 G34W-positive cells were scattered around the strand-like matrix; however, the number of H3.3 G34W-positive stromal cells was reduced markedly compared to the other soft tissue lesion in which osteoclastic giant cells persisted. In the lesion presenting with persistent osteoclastic giant cells, H3.3 G34W-positive cells comprised up to 70% of stromal cells (Figure 3B′). We conclude that the response to denosumab treatment was associated with a change of morphology characterized by a reduction in both osteoclastic giant cells and H3.3 G34W-positive stromal cells along with increasing formation of strand-like osteoid (Figure 3B–C′).

Table 1. Clinical, H3F3A mutation and immunohistological data of giant all tumour of the bones

Case	Diagnosis	Age	Sex	Localization	H3F3A PCR/Seq	G34W IHC
1	GCTB	42	F	Head of right tibia	Mut p.G34W	+
2	GCTB	35	M	Left proximal humerus	Mut p.G34W	+
3	GCTB	17	M	Head of left fibula	Mut p.G34W	+
4	GCTB	54	M	Head of left proximal humerus	Mut p.G34W	+
5	GCTB	23	M	Left distal femur	Mut p.G34W	+
6	GCTB	50	F	Head of left fibula	Mut p.G34W	+
7	GCTB	48	M	Right tibia	Mut p.G34W	+
8	GCTB	34	M	Right distal femur	Mut p.G34W	+
9	GCTB	35	M	Right distal femur	Mut p.G34W	+
10	GCTB	63	F	Left tibia	Mut p.G34W	+
11	GCTB	52	F	Head of right tibia	Mut p.G34W	+
12	GCTB	46	M	Left distal femur	Mut p.G34W	+
13	GCTB	81	M	Left lateral ankle	Mut p.G34W	+
14	GCTB	42	M	Head of right fibula	Mut p.G34W	+
15	GCTB	52	M	Right proximal humerus	Mut p.G34W	+
16	GCTB	33	F	Right spina iliaca anterior superior	Mut p.G34W	+
17	GCTB	24	M	Head of right humerus	Mut p.G34W	+
18	GCTB	17	F	Proximal left tibia	Mut p.G34W	+
19	GCTB	53	M	Distal left radius	Mut p.G34W	+
20	GCTB	50	F	Head of left fibula	Mut p.G34W	+
	Resection			Head of left fibula	WT	+
21	GCTB	41	M	Thumb (metacarpal bone) of left hand	WT	+
	Resection			Metacarpal I region of left hand	Mut p.G34W	+
22	GCTB	28	F	Lateral condyle of left femur	Mut p.G34W	+
	Recurrence 1			Local recurrence on left femur	Mut p.G34W	+
	Recurrence 2			Local recurrence on left femur	Mut p.G34W	+
	Metastasis			Left lung, segment VI of lower lobe	Mut p.G34W	+
	Resection			Distal left femur	Mut p.G34W	+

GCTB, giant cell tumour of bone; M, male; F, female; PCR, polymerase chain reaction; Seq, sequencing; Mut, mutation; WT, wild-type; IHC, immunohistochemistry; +, positive.

Discussion

Giant cell tumour of the bone is a primary bone lesion characterized by a neoplastic population of mononuclear cells with interspersed osteoclastic giant cells. A driver mutation H3F3A G34W has been described that allows GCTB to be distinguished from other giant cell-containing lesions that have to be considered.[4,6,11]

Here, we show that nuclear staining of the mononuclear compartment of GCTB was detected exclusively in mononuclear stromal cells of H3F3A-

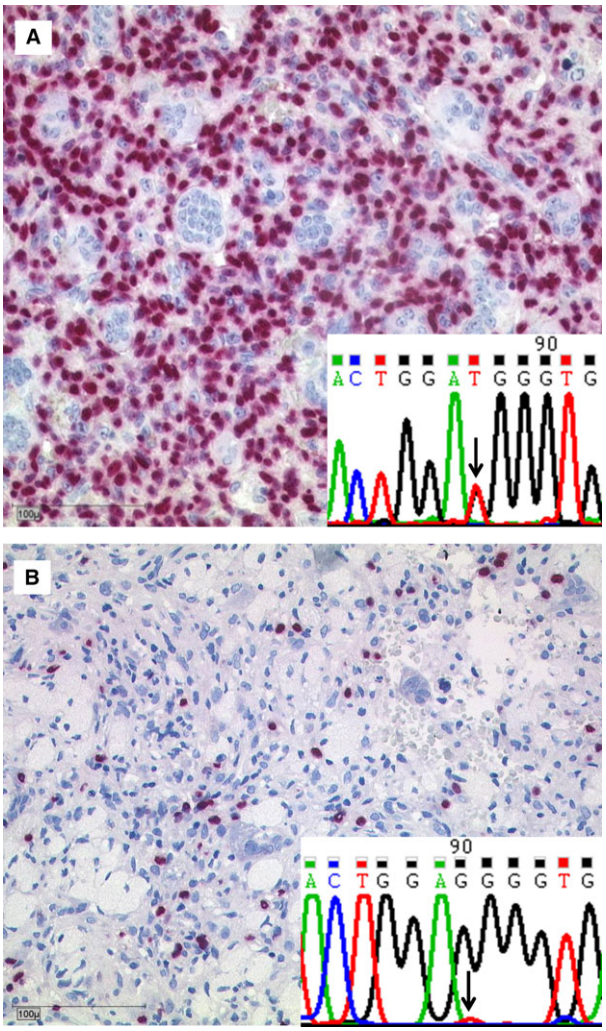

Figure 1. Detection of the H3F3A mutation in giant cell tumour of the bone (GCTB). **A**, Expression of G34W in a H3F3A mutated GCTB (case 17) with strong nuclear positivity in the stromal compartment, while osteoclastic giant cells are negative; insert shows corresponding Sanger sequencing profile with a high mutational peak (arrow) masking the wild-type peak (black line). **B**, Expression of G34W in a GCTB (case 20, resection specimen). Only a few tumour cells are positive for G34W; note the diminished mutational peak covered by a predominating wild-type peak in the insert.

mutated tumours. We found that the osteclastic giant cells within the mutated samples showed no nuclear reactivity, confirming the concept that these cells are induced by an abnormal production of receptor activator of nuclear factor κB (RANK) ligand of the neoplastic mononuclear component.[15] All other samples of giant cell-containing bone and soft tissue lesions analysed by means of Sanger sequencing and IHC proved to be negative for the H3F3A mutation. Therefore, positive staining for H3.3 G34W in IHC is an indicator of the H3F3A mutation in GCTB.

This mutation has been described in GCTB within a frequency range of 69–96%.[4,6] Alternatively, in one of 53 cases of GCTB reported by Behjati *et al.* there was an H3F3A mutation in the same exon, leading to a substitution of glycine 34 for leucine (G34L). Moreover, some very rare GCTB without any detectable driver mutation have been described. Conversely, one OS and one high-grade osteoclast-rich tumour with adamantinoma-like features have been found to also harbour the G34W mutation.[11,16] Therefore, negative staining in H3.3 G34W IHC does not rule out GCTB completely, and positive staining always has to be interpreted in the context of clinical features, radiographic imaging and histomorphology.

Mutation analysis for specific point mutations is generally achieved using PCR and sequencing techniques such as Sanger sequencing. This last method has been shown to detect mutations even when the tumour cell burden in a given sample is as low as 6.6%. However, Sanger sequencing is not always available to diagnostic laboratories. Furthermore, conventional DNA analysis remains expensive and takes a minimum of a week.[17]

We analysed three patients with several disease recurrences. All recurrences were analysed for the specific H3F3A mutation although, in some instances, the mutations were not detectable by means of PCR and Sanger sequencing. This might be due to the low tumour cell content. On re-analysis of these samples using IHC we actually found that the number of H3.3 G34W-positive tumour cells was clearly lower compared to samples with an unequivocally positive sequencing result and a higher number of positive cells in IHC. Given that callus formation and fibrosis may diminish further the absolute number of tumour cells, especially on small tumour biopsies taken during curettage, the power of the IHC staining for H3.3 G34W might be even higher than mutational sequencing analysis alone in some cases; this is of interest, as the limited sensitivity of Sanger sequencing regarding H3F3A mutation analysis has been discussed previously and the method remains expensive and time-consuming in comparison.[6,13,17] Due to the fact that all H3F3A-positive samples showed specific staining after both acid-based and EDTA decalcification, standard immunohistochemical staining is a highly reliable and robust method for detecting the H3F3A mutation using the H3.3 G34W mutant mAb as a tool for GCTB diagnosis.

Chondroblastomas are characterized by the mutation K36M of the H3F3B gene. This mutation can be detected reliably at the protein level by a monoclonal antibody detecting the mutational site H3.3 K36M,

Table 2. Clinical and immunohistological data of H3F3A wild-type giant cell lesion of bone and soft tissue

Case	Diagnosis	Age	Sex	Localization	H3F3A PCR/Seq	G34W IHC
1	Brown tumour	19	M	Right femur and tibia	WT	–
1	ABC	42	F	Metatarsal bone	WT	–
2	ABC	18	F	Left dorsal femur	WT	–
3	ABC	45	M	D5 of left hand	WT	–
4	ABC	20	M	Cervical vertebra	WT	–
5	ABC	10	M	Distal right tibia	WT	–
6	ABC	11	M	Distal right humerus	WT	–
1	Chondroblastoma	13	F	Left proximal tibia	NA	–
2	Chondroblastoma	15	M	Left medical femur condyle	NA	–
3	Chondroblastoma	19	F	Left acetabular region	NA	–
4	Chondroblastoma	16	M	Medial condyle of left femur	NA	–
5	Chondroblastoma	20	M	Head of right humerus	NA	–
6	Chondroblastoma	21	M	5th right rib	WT	–
1	NOF	16	M	Distal left tibia	NA	–
2	NOF	16	F	Metaphysis of right femur	NA	–
3	NOF	14	F	Distal right tibia	NA	–
4	NOF	10	F	Distal right femur	NA	–
5	NOF	35	F	Pubic bone	WT	–
1	Fibrous dysplasia	10	F	Proximal humerus	WT	–
2	Fibrous dysplasia	73	F	Right radius	WT	–
1	TSGCT	83	F	Right shoulder joint	WT	–
2	TSGCT	43	M	Left thigh	WT	–
3	TSGCT	29	F	Left upper ankle joint	WT	–
4	TSGCT	49	F	Soft tissue around left radius	WT	–
5	TSGCT	54	M	Left dorsal knee	WT	–
6	TSGCT	72	F	Left knee	WT	–
7	TSGCT	50	M	D3 of left hand	WT	–
8	TSGCT	48	M	Left knee	WT	–
9	TSGCT	33	F	Left knee	WT	–
1	GC rich sarcoma	62	M	Left distal femur	WT	–
2	Osteosarcoma (NOS)	20	M	Right femur	NA	–
3	Chondroblastic osteosarcoma	16	M	Upper aperture of thorax	WT	–
4	Osteoblastic osteosarcoma	23	M	Left proximal femur	WT	–
5	Osteoblastic osteosarcoma	27	F	Left femur	WT	–

Table 2. *(Continued)*

Case	Diagnosis	Age	Sex	Localization	H3F3A PCR/Seq	G34W IHC
6	Osteoblastic osteosarcoma	48	M	Right proximal tibia	WT	–
7	Osteoblastic osteosarcoma	38	M	Left tibia	WT	–

ABC, aneurysmal bone cyst; NOF, non-ossifying fibromas; TSGCT, tenosynovial giant cell tumour; M, male; F, female; PCR, polymerase chain reaction; Seq, sequencing; GC, giant cell; WT, wild-type; IHC, immunohistochemistry; NA, not analysed; –, negative.

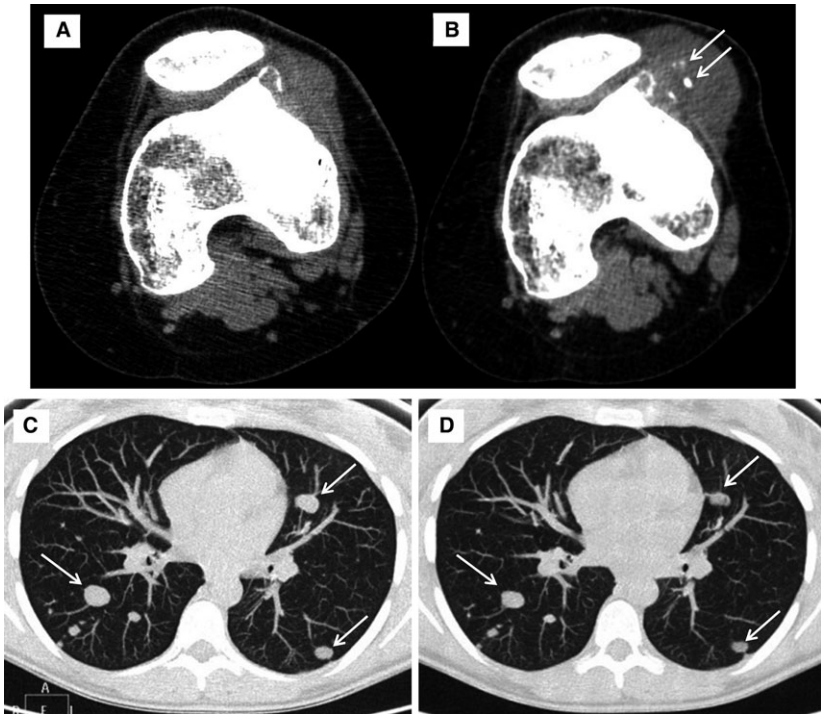

Figure 2. Radiographic imaging of case 22. **A, B,** Computed tomography scans without contrast medium. First scan (G) taken 3 months before the start of therapy. Second scan (H) after administration of three injections of denosumab. Comparison reveals small calcifications (arrows) in the extra-osseous part of the giant cell tumour of the bone (GCTB); tumour size is not diminished. **C, D,** Computed tomography scans of the lungs show multiple round lesions before (**C**) and after (**D**) three courses of denosumab treatment; lung metastases show a moderate reduction in size (arrows).

as has been shown previously.[13] All chondroblastomas tested with this antibody in our study showed strong nuclear staining, confirming this finding. Of note, these chondroblastomas were negative for staining with the monoclonal antibody H3.3 G34W specific for GCTB (Supporting information, Figure S1A, A′).

Therefore, these findings confirm the discriminative power of the immunohistological approach to detecting and distinguishing these two histone point mutations.

We had the opportunity to analyse samples obtained from a patient with GCTB of the distal left femur with disseminated spread to the lungs as the disease took a rare malignant course.[7] IHC staining against H3.3 G34W of the lung biopsy confirmed metastatic spread of the tumour to the lungs. Hence, the H3.3 G34W detecting antibody can be seen as a valuable tool to detect GCTB wherever it occurs.

The patient received four injections of denosumab (Xgeva®). This treatment has become a standard therapy for advanced or inoperable GCTB.[18–21] Histologically, denosumab had induced dramatic changes to the GCTB after four injections administered over a period of 8 weeks. These were characterized by areas consisting of spindle-shaped tumour cells with an interspersed matrix. In these areas, giant cells were reduced markedly. In the areas poor in osteoclastic giant cells we saw intermingled strand-like structures consisting of connective tissue. The cells adjacent to these trabeculae were negative for H3.3 G34W IHC staining. This depicts a dramatic change in histomorphology of GCTB on denosumab treatment, leading to replacement of the mutated cells by reactive fibroblasts and/or osteoblasts that are negative for staining.

This finding may support the view that denosumab treatment promotes a reactive, H3F3A wild-type population to produce calcifying connective tissue and

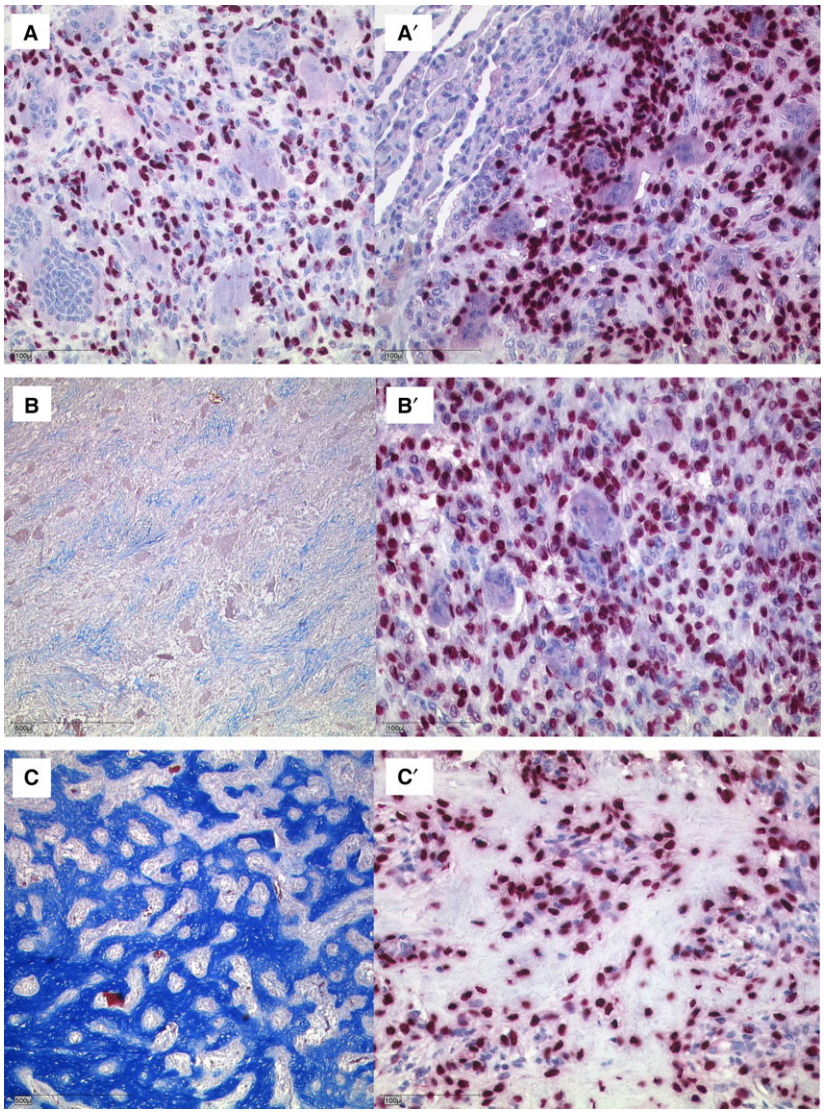

Figure 3. Histology of case 22. **A**, The primary tumour shows a strong nuclear positivity for the H3.3 G34W detecting antibody in the nuclei of the stromal compartment. Osteoclastic giant cells are negative. **A′**, Expression of H3.3 G34W in a pulmonary metastasis; pulmonary parenchyma (upper left part) is negative. **B, B′**, Histological aspects of tumour samples after denosumab therapy in an Azan histochemical staining; only modest amounts of connective tissue are present while osteoclastic giant cells persist (**B**). The same area of the tumour shows a high number of G34W-positive tumour cells (**B′**). **C, C′**, Azan staining reveals strand-like formation of osteoid (**C**); the number of G34W tumour cells is reduced in this area (**C′**) compared to Figure B′. Osteoclastic giant cells are not detected (bars in **A, A′, B′, C′** = 100 μm; bars in **B** and **C** = 500 μm).

leads ultimately to very dense bone, as described previously.[18] Therefore, staining with the monoclonal antibody detecting the mutation H3.3 G34W confirms that the tumour cells of GCTB persist in low numbers on denosumab treatment, while reactive mesenchymal cells start to produce fibrous matrix and osteoid.

In conclusion, we show that GCTB can be diagnosed by the monoclonal antibody (clone RM263) detecting the H3.3 G34W mutation. This antibody is a valuable immunohistological tool in histological differential diagnosis of giant cell-containing lesions of the bone and soft tissue. Furthermore, the antibody proves that denosumab (Xgeva®) leads to a dramatic change of the histomorphology of the tumour with a decreased number of tumour cells accompanied by loss of osteoclastic giant cells and the appearance of reactive mesenchymal cells inducing local fibrosis and osteoid.

Acknowledgements

We thank Juliane Nell, Michaela Buck, Ulrike Kostezka and Elena Moser for excellent technical assistance. Case 22 was presented at the 86th meeting of the Arbeitsgemeinschaft Knochentumouren e.V./ Working Group on Bone Tumours in Trier, Germany, 22–23 April 2016, and received the AGKT award as best presentation. Funding source for this work was a scholarship in experimental medicine granted to cand. med. Julian Lüke by the University of Ulm. The

monoclonal antibody against the mutational site H3.3 G34W (clone RM263) was provided by RevMab Biosciences as a gift and for evaluation.

Conflicts of interest

The authors declare no conflicts of interest.

References

1. World Health Organization. *Pathology and genetics of tumours of soft tissue and bone*. Lyon: IARC, 2017.
2. Werner M. Giant cell tumour of bone: morphological, biological and histogenetical aspects. *Int. Orthop.* 2006; **30**; 484–489.
3. Wulling M, Engels C, Jesse N *et al.* The nature of giant cell tumour of bone. *J. Cancer Res. Clin. Oncol.* 2001; **127**; 467–474.
4. Presneau N, Baumhoer D, Behjati S *et al.* Diagnostic value of H3F3A mutations in giant cell tumour of bone compared to osteoclast-rich mimics. *J. Pathol. Clin. Res.* 2015; **1**; 113–123.
5. Alix-Panabieres C, Arlt MJE, Bataille R *et al.* List of contributors. In: Heymann D ed. *Bone cancer* (Second edition). San Diego: Academic Press, 2015; 257–272.
6. Cleven AH, Hocker S, Briaire-de Bruijn I *et al.* Mutation analysis of H3F3A and H3F3B as a diagnostic tool for giant cell tumour of bone and chondroblastoma. *Am. J. Surg. Pathol.* 2015; **39**; 1576–1583.
7. Muheremu A, Niu X. Pulmonary metastasis of giant cell tumour of bones. *World J. Surg. Oncol.* 2014; **12**; 261.
8. Czerniak B, Dorfman HD. *Dorfman and Czerniak's bone tumours*. St Louis, MO: Elsevier, 2015.
9. Dominkus M, Ruggieri P, Bertoni F *et al.* Histologically verified lung metastases in benign giant cell tumours – 14 cases from a single institution. *Int. Orthop.* 2006; **30**; 499–504.
10. Yuen BT, Knoepfler PS. Histone H3.3 mutations: a variant path to cancer. *Cancer Cell* 2013; **24**; 567–574.
11. Behjati S, Tarpey PS, Presneau N *et al.* Distinct H3F3A and H3F3B driver mutations define chondroblastoma and giant cell tumour of bone. *Nat. Genet.* 2013; **45**; 1479–1482.
12. Dtsch Arztebl 2003; 100: A 1632 [Heft 23]. Available at http://m.aerzteblatt.de/print/37253.html. Accessed 9 February 2017.
13. Amary MF, Berisha F, Mozela R *et al.* The H3F3 K36M mutant antibody is a sensitive and specific marker for the diagnosis of chondroblastoma. *Histopathology* 2016; **69**; 121–127.
14. Ellegast J, Barth TF, Schulte M *et al.* Metastasis of osteosarcoma after 16 years. *J. Clin. Oncol.* 2011; **29**; e62–e66.
15. Boyce BF, Xing L. Functions of RANKL/RANK/OPG in bone modeling and remodeling. *Arch. Biochem. Biophys.* 2008; **473**; 139–146.
16. Joseph CG, Hwang H, Jiao Y *et al.* Exomic analysis of myxoid liposarcomas, synovial sarcomas, and osteosarcomas. *Genes Chromosom. Cancer* 2014; **53**; 15–24.
17. Ihle MA, Fassunke J, Konig K *et al.* Comparison of high resolution melting analysis, pyrosequencing, next generation sequencing and immunohistochemistry to conventional Sanger sequencing for the detection of p. V600E and non-p.V600E BRAF mutations. *BMC Cancer* 2014; **14**; 13.
18. Branstetter DG, Nelson SD, Manivel JC *et al.* Denosumab induces tumour reduction and bone formation in patients with giant-cell tumour of bone. *Clin. Cancer Res.* 2012; **18**; 4415–4424.
19. Balke M. Denosumab treatment of giant cell tumour of bone. *Lancet Oncol.* 2013; **14**; 801–802.
20. Balke M, Hardes J. Denosumab: a breakthrough in treatment of giant-cell tumour of bone? *Lancet Oncol.* 2010; **11**; 218–219.
21. Balke M, Schremper L, Gebert C *et al.* Giant cell tumour of bone: treatment and outcome of 214 cases. *J. Cancer Res. Clin. Oncol.* 2008; **134**; 969–978.

Supporting Information

Additional Supporting Information may be found in the online version of this article:

Figure S1. Immunohistology of a chondroblastoma and a non-ossifying fibroma **A, A′,** A chondroblastoma with typical cartilaginous matrix and some giant cells is G34W-negative. **B, B′,** A non-ossifying fibroma with spindle cells and intermingled giant cells is G34W-negative.